

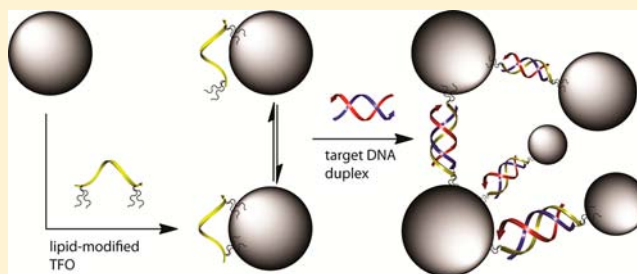
# Assembly of Liposomes Controlled by Triple Helix Formation

Ulla Jakobsen and Stefan Vogel\*

Nucleic Acid Center, Department of Physics, Chemistry and Pharmacy, University of Southern Denmark, Campusvej 55, 5230 Odense M, Denmark

**S** Supporting Information

**ABSTRACT:** Attachment of DNA to the surface of different solid nanoparticles (e.g., gold and silica nanoparticles) is well established, and a number of DNA-modified solid nanoparticle systems have been applied to thermal denaturation analysis of oligonucleotides. We report herein the noncovalent immobilization of oligonucleotides on the surface of soft nanoparticles (i.e., liposomes) and the subsequent controlled assembly by DNA triple helix formation. The noncovalent approach avoids tedious surface chemistry and necessary purification procedures and can simplify and extend the available methodology for the otherwise difficult thermal denaturation analysis of complex triple helical DNA assemblies. The approach is based on lipid modified triplex forming oligonucleotides (TFOs) which control the assembly of liposomes in solution in the presence of single- or double-stranded DNA targets. The thermal denaturation analysis is monitored by ultraviolet spectroscopy at submicromolar concentrations and compared to regular thermal denaturation assays in the absence of liposomes. We report on triplex forming oligonucleotides (TFOs) based on DNA and locked nucleic acid (LNA)/DNA hybrid building blocks and different target sequences (G or C-rich) to explore the applicability of the method for different triple helical assembly modes. We demonstrate advantages and limitations of the approach and show the reversible and reproducible formation of liposome aggregates during thermal denaturation cycles. Nanoparticle tracking analysis (NTA) and dynamic light scattering (DLS) show independently from ultraviolet spectroscopy experiments the formation of liposome aggregates.



## INTRODUCTION

Hybridization assays based on thermal denaturation experiments are widely used tools for the understanding of fundamental structural changes during hybridization of oligonucleotides. Experimental data, such as thermal denaturation temperatures and characteristic curve shapes obtained by monitoring the thermal cycling of DNA double or triple helices by spectroscopic methods,<sup>1</sup> are of importance for the development and improvement of diagnostic assays<sup>2–5</sup> (e.g., for detection of single nucleotide polymorphisms, deletions, or insertions).<sup>2,3</sup>

Whereas thermal denaturation analysis is established as a standard tool for characterization of double helices, the thermal denaturation analysis of triple helical structures is limited by the nature of triplex forming oligonucleotides (TFOs) and can be complicated due to, e.g., lack of thermal transitions for triplex melting,<sup>6–9</sup> or overlap between triplex and duplex melting transitions.<sup>10–16</sup> Furthermore, self-association by one or more of the strands<sup>6,17–19</sup> to form, e.g., i-motifs,<sup>11,20–22</sup> parallel homoduplexes,<sup>6,7,18,23,24</sup> and guanine quartets,<sup>20</sup> can also give rise to thermal transitions. It would therefore be of great interest to differentiate alternative motifs and self-complementary sequences from the formation of triple helices in a simple denaturation assay. We recently reported the DNA-controlled assembly of soft nanoparticles (liposomes) by DNA-duplex formation. DNA strands modified at both ends with lipophilic substituents are able to induce aggregation of liposomes upon

formation of double helices with unmodified, complementary strands.<sup>25,26</sup> The assembly process requires only one terminally modified probe strand and results in highly sequence specific assembly of liposomes, which can be used as a simple readout system during thermal denaturation experiments. Standard thermal denaturation experiments monitor the hyperchromatic behavior of oligonucleotides as optical readout and consequently require oligonucleotides in micromolar concentrations,<sup>1</sup> whereas the assembly of liposomes is based on the scattering of light, requires only nanomolar concentrations, and is not limited to specific wavelengths.<sup>25,26,38,59</sup> The extension of this strategy to a much more complex system using triple helices to assemble liposomes (Figure 1) will be described here. We have focused on analytical applications for thermal denaturation assays and investigated important parameters of the TFO design such as probe sequences (G or C-rich), and alternative DNA building blocks (i.e., locked nucleic acids – LNA versus DNA) but not further investigated the morphology of the resulting aggregates. This was justified by earlier investigations by us which have shown that the individual liposomes remain largely unaltered during the reversible assembly process; no DNA-induced liposome fusion occurs for our lipid-modified DNA-probe design (probe length >8-

**Received:** January 8, 2013

**Revised:** July 15, 2013

**Published:** July 25, 2013

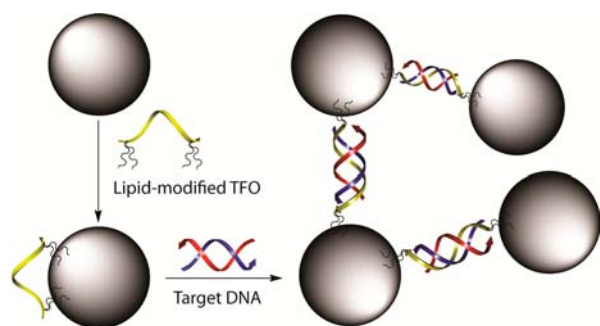


**Figure 1.** Schematic representation of DNA-controlled assembly of liposomes by triple helix formation. Oligonucleotides (red, blue, and yellow ribbons) and liposomes (gray spheres) are not drawn to scale. A number of triple helices are necessary to hold two liposomes together (not shown for simplicity).

mers) and no content leakage is observed ( $\text{Ca}^{2+}$ /arsenazo III assay).<sup>25,26</sup>

Triple helices can be formed when a triplex-forming oligonucleotide (TFO) binds in the major groove of a double helix with an appropriate sequence (one homopurine and one homopyrimidine strand) by formation of Hoogsteen base pairs,<sup>27</sup> and can be classified as parallel or antiparallel depending on the orientation of the TFO relative to the purine-rich strand of the duplex. For parallel triplexes, the TFO is pyrimidine-rich and bound by Hoogsteen hydrogen bonds. The formation of triplexes containing a large amount of  $\text{T} \times \text{A} \cdot \text{T}$  and  $\text{C}^+ \times \text{G} \cdot \text{C}$  triplets is dependent on pH due to the need for protonation of cytidine,<sup>28</sup> but  $\text{G} \times \text{G} \cdot \text{C}$  triplets can also be part of a TFO with parallel orientation.<sup>28–30</sup> Antiparallel triplexes are formed with a purine-rich TFO and contain  $\text{G} \times \text{G} \cdot \text{C}$ ,  $\text{A} \times \text{A} \cdot \text{T}$ , or  $\text{T} \times \text{A} \cdot \text{T}$  triplets stabilized by reverse Hoogsteen hydrogen bonds.<sup>28</sup> Triplex structures have previously been used for assembly of gold nanoparticles by using a hairpin duplex and a TFO both attached to gold nanoparticles,<sup>31,32</sup> a TFO split into two LNA- and 5-methyldeoxycytidine modified oligonucleotides attached to gold nanoparticles, and an unmodified duplex<sup>33</sup> or two gold nanoparticle modified oligonucleotides, one unmodified oligonucleotide, and triplex-binders.<sup>34</sup> Also, single-walled carbon nanotubes covalently attached to oligonucleotides have been assembled by triple helices in the presence of the triplex formation inducer coralyne.<sup>35</sup> However, assembly of nanostructures using three strands without triplex-binders or assembly of soft nanoparticles (liposomes) has not previously been reported. Furthermore, this is to the best of our knowledge also the first example of triplex-mediated assembly of nanoparticles using only one modified strand (namely the TFO) and an unmodified duplex target.

## ■ EXPERIMENTAL PROCEDURES

**Reagents.** All reagents and solvents were purchased commercially and used without further purification. Milli-Q water was used in all experiments. Unmodified oligonucleotides were purchased from Sigma-Aldrich.

**Instrumentation.** Modified oligonucleotides were synthesized on an Expedite 8900 nucleic acid synthesis system (Perceptive Biosystems Inc.). HPLC purification of oligonucleotides was performed on a Dionex Ultimate 3000 with a DIONEX Acclaim C18 3  $\mu\text{m}$  300 Å reverse phase column. Mass spectra were recorded on a Bruker Daltonics microflex

LT MALDI-TOF. Liposomes were extruded with a LIPEX Extruder (Northern Lipids). Thermal denaturation studies were carried out on a Varian Cary 100 Bio UV–visible spectrophotometer or a Varian Cary 3E UV–visible spectrophotometer with a Peltier controlled  $6 \times 6$  sample changer and Cary WinUV software. Dynamic light scattering was measured using a Brookhaven BI-200SM with a 632 nm laser diode. Nanoparticle tracking analysis measurements were performed with a NanoSight LM10-HS equipped with an Andor Lucas EMCCD camera and a LM14 temperature controller and a laser diode operated at 404 nm. The data was analyzed using the NanoSight NTA 2.1 software.

**Synthesis of Oligonucleotides.** The lipid modified phosphoramidite was synthesized and incorporated in oligonucleotides as previously described.<sup>25,26</sup> The synthesized oligonucleotides were purified as previously described.<sup>26</sup> Briefly, the HPLC system was used with UV detection at 260 nm and a flow of  $1 \text{ mL min}^{-1}$  with the following gradient program for lipid-modified oligonucleotides: 2 min isocratic with 0.05 M triethylamine ammonium acetate (TEAA) (buffer A) followed by a 8 min linear gradient to 70% 1:3  $\text{H}_2\text{O}:\text{MeCN}$  (buffer B), which was increased to 100% over 20 min and then continued for 30 min. LNA-modified oligonucleotides without lipid modifications were purified using the following gradient program: 2 min isocratic A, followed by a 38 min linear gradient to 50% B. The identity of the synthesized oligonucleotides was verified by mass spectrometry (Supporting Information).

**Preparation of Liposomes.** 1-Palmitoyl-2-oleyl-*sn*-glycero-3-phosphocholine (POPC) was suspended in 20 mM sodium cacodylate buffer, 110 mM NaCl, 10 mM  $\text{MgCl}_2$ , pH 6.0 at a concentration of 10 mM. The solution was extruded 10 times through double polycarbonate filters with a 50 nm pore size using compressed  $\text{N}_2$  (20–40 bar).

**$T_m$  Measurements.** Thermal melting curves were obtained by recording the absorbance of samples at 260 nm as a function of the temperature from 15 to 90 °C at a rate of  $0.5 \text{ }^\circ\text{C min}^{-1}$  for measurements with liposomes and from 10 to 90 °C at a rate of  $1 \text{ }^\circ\text{C min}^{-1}$  for measurements without liposomes. Prior to melting experiments, an annealing step consisting of heating the samples once to 90 °C and then cooling to the starting temperature at a rate of  $10 \text{ }^\circ\text{C min}^{-1}$  was performed. For measurements with liposomes, the same samples were repeatedly heated and cooled 3 times, and before each cycle the samples were kept at 15 °C for 30 min. For measurements without liposomes, the samples were kept at 10 °C for 30 min before the measurements were started. The melting temperatures were determined as the maximum of the first derivative of the melting curves for measurements without liposomes and as the minimum for measurements with liposomes. The melting temperatures were recorded in 20 mM sodium cacodylate buffer with 100 mM NaCl, 10 mM  $\text{MgCl}_2$ , and pH 5.0, 6.0, and 7.2. A concentration of 1.0  $\mu\text{M}$  of the duplex target was used for measurements without liposomes, and 0.05 and 0.1  $\mu\text{M}$  was used for measurements with liposomes. In all measurements with three strands, 1.5 equiv of the TFOs were used, and for measurements with only two DNA strands, equimolar concentrations of the two strands were added. For measurements with only lipid-modified TFOs with liposomes, DNA concentrations of 0.05, 0.75, 0.1, and 0.15  $\mu\text{M}$  were tested. For thermal denaturation experiments with liposomes, liposomes were added to a final POPC concentration of 0.5 mM. All melting temperatures (Supporting Information) are

reported with an uncertainty of  $\pm 1$  °C as determined from multiple experiments. However, melting temperatures for lipid-modified oligonucleotides without liposomes are reported with greater uncertainty due to the broad and nonideal melting curves often obtained for such oligonucleotides.<sup>60</sup>

**Dynamic Light Scattering.** Samples containing 0.1  $\mu$ M double helix, 0.15  $\mu$ M TFO, and liposomes (0.5 mM POPC) in 20 mM sodium cacodylate buffer with 100 mM NaCl, 10 mM  $MgCl_2$ , and pH 5.0 were heated and cooled repeatedly three times as described for  $T_m$  measurements before use for dynamic light scattering measurements. Each sample was prepared and measured in duplicate.

**Nanoparticle Tracking Analysis (NTA).** Samples were heated and cooled repeatedly three times as described for  $T_m$  measurements. Due to the relatively low particle concentration necessary for NTA ( $10^8$ – $10^9$  particles/mL), the samples were then diluted 20-fold with buffer (20 mM sodium cacodylate buffer with 100 mM NaCl, 10 mM  $MgCl_2$ , and pH 5.0) prior to measurements, except for samples containing three different DNA strands (triple helices) which were diluted 50-fold. The measurements were carried out at 20 °C and with 2049 frames/120 s capture duration. All samples were prepared in duplicate and each of these samples was measured twice. The recorded videos were analyzed using a minimum expected particle size of 50 nm, a screen gain of 3,  $3 \times 3$  blur, and a detection threshold of 5 for samples containing no, one, or two different oligonucleotide strands and a detection threshold of 20 for samples containing triple helices. For all analytical methods used, a number of control experiments have been performed to exclude unspecific aggregation of POPC liposomes by the buffer used; none of the control experiments have shown aggregation of liposomes.

## RESULTS AND DISCUSSION

In the system presented here, the TFOs are modified with lipid substituents at both ends, and consequently no surface chemistry is needed, as the TFOs will adhere to the liposome surface when mixed with these without the need to purify the resulting nanoparticle–oligonucleotide conjugates. As the TFOs are noncovalently attached to the liposomes, they can move freely on the surface of the membranes as reported for vesicles tethered by DNA to supported lipid bilayers<sup>36,37,62</sup> and the attachment of the oligonucleotides to the liposomes does not affect their ability to hybridize with complementary sequences.<sup>25,26,38</sup> Furthermore, the noncovalently attached oligonucleotides are expected to be more accessible, less restricted in respect to overall movement, and less sterically blocked than covalently bound oligonucleotides. Since only the TFO is modified, it is only necessary to synthesize one modified oligonucleotide to be able to test, e.g., other sequence designs. The lipophilic modification used for the experiments presented here consists of two palmitoyl chains attached to a crown ether scaffold (X, Scheme 1) and can be inserted in oligonucleotides by the phosphoramidite method in high yield.<sup>39</sup>

The principle of the assembly is analogous to the principle described for liposome-assembly controlled by DNA duplex formation,<sup>25,26</sup> but for the triplex-controlled liposome assembly, the highly increased steric demands and charge accumulation require the assembly principle to be very robust and a very strong driving force for the assembly to occur (Figure 1). TFOs modified with membrane anchors at both ends adhere (anchor) strongly to the surface of liposomes. This adhesion of the

## Scheme 1. Structure of Membrane Anchor X and DNA Sequences for Duplex Targets and TFOs

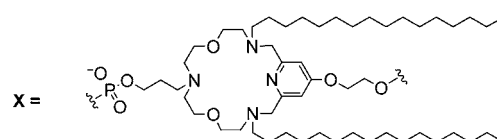
### Duplex targets:

**16D** 3'-TTTTCTTTCCCCCT  
5'-AAAAGAAAAGGGGGA

**47D** 3'-CATCTAGAATCGGTGAAAAATTTCTTTCCCCCTGACCTTCCGA  
5'-GTAGATCTTAGCCACTTTTTAAAGAAAAGGGGGGACTGGAAGGGCT

### Triplex forming oligonucleotides:

**TFO-C** 5'-TTTXXXXTTTCCCCCTXTT  
**TFO-G** 5'-TTTXXXXTTTGGGGGTXTT  
**TFO-C<sub>L</sub>** 5'-TTTXXTTTCTTTTCCCCCTXTT  
**TFO-G<sub>L</sub>** 5'-TTTXXTTTCTTTTGGGGGTXTT



membrane anchors is a dynamic and generally reversible process, but the four hydrophobic alkyl chains (two at each end of the TFO) ensure that the oligonucleotides are irreversibly attached (attachment is concentration independent for bivalent anchoring).<sup>61</sup> However, the lipid chains at either end of the TFO are able to leave the membrane partially and thus enable hybridization to occur. The irreversible attachment (practically no partitioning into solution for bivalent membrane anchoring with two membrane anchors<sup>25</sup>) of lipid-modified oligonucleotides has been shown in comprehensive studies earlier<sup>37,61</sup> and further substantiated by liposome assembly studies with membrane anchor X on immobilized bilayers.<sup>25</sup> When an oligonucleotide duplex with a sequence appropriate for triplex formation is added, the lipid-modified TFO binds in the major groove of the duplex. The resulting triple helix is very rigid, for which reason it is no longer possible for the membrane anchors at both ends of the TFO to be anchored to the same liposome. One of the ends will therefore adhere to another liposome during triplex formation resulting in formation of liposome aggregates. Hybridization induced formation of interliposomal linkages (liposome aggregation) is caused by continuously increased pull by the target oligonucleotide duplex while hybridizing to the membrane anchored probe, resulting in a final detachment of one of the terminal double anchoring units (X). A number of triple helices are needed to link two liposomes as seen for double helices from calculations based on DNA concentrations in solution and literature reports on DNA-controlled assembly of gold nanoparticles.<sup>53</sup> The formation of the aggregates is a reversible process and the aggregates disassemble when heated to above the melting temperature of the triplex, but are reformed upon cooling. As the aggregates are significantly larger than the individual liposomes, they scatter light considerably more, and this property can be utilized to follow the assembly and disassembly process, e.g., by UV spectroscopy or dynamic light scattering (DLS) at different wavelengths.<sup>25,26</sup>

A sequence related to the human immunodeficiency virus (HIV) type 1 polypurine tract (PPT) was chosen as duplex target, as this sequence is known to participate in triple helix formation, and both the 16-base pair long tract<sup>40</sup> (16D) as well as a longer sequence with overhangs<sup>41</sup> (47D) were tested (Scheme 1). To evaluate both a pH-dependent and -independent TFO, two different probe sequences were



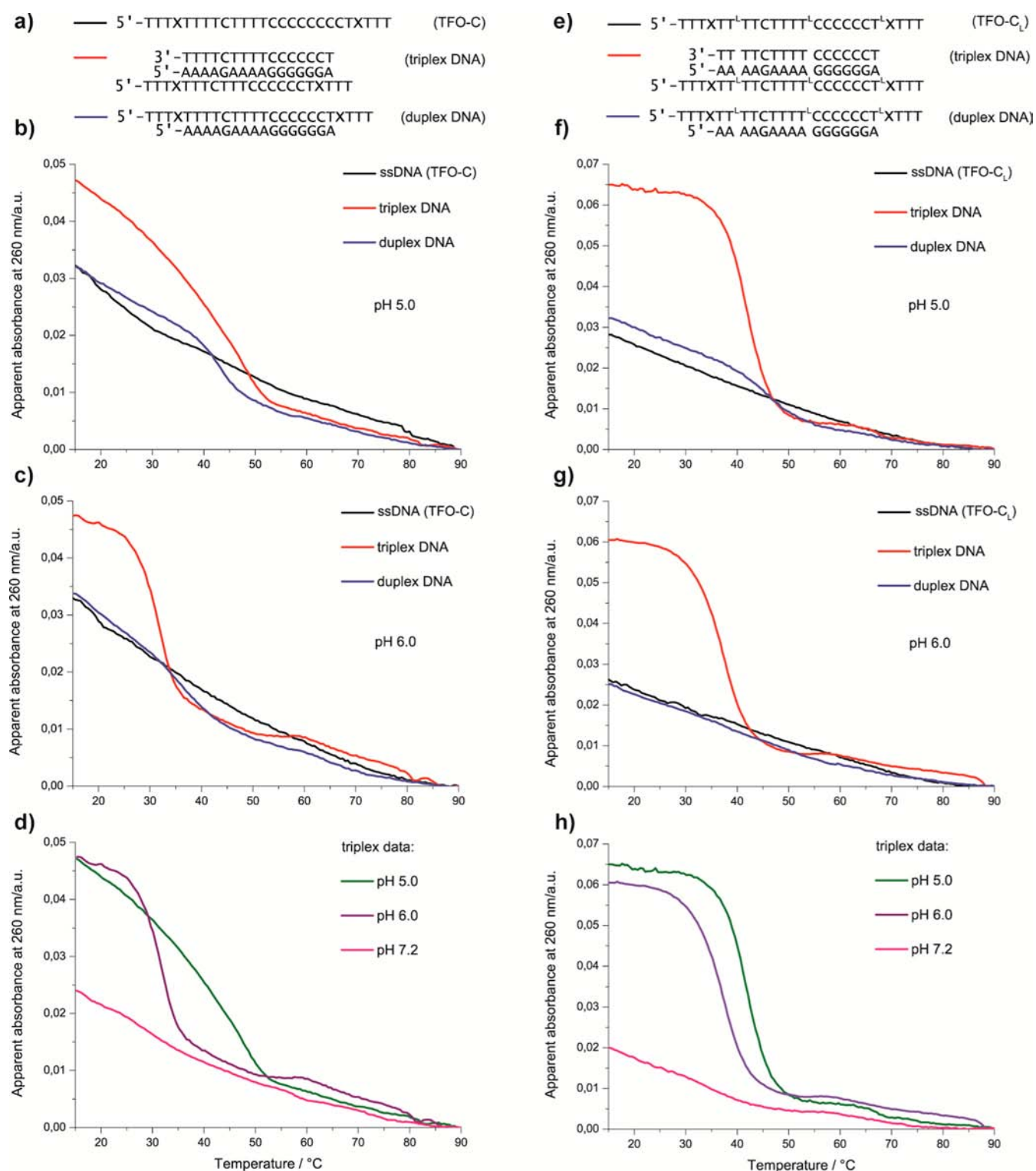


**Figure 2.** Second heating curves for TFO-C and TFO-C<sub>L</sub> in the presence of liposomes (black curve in parts b, c, f, g) and with one (blue curve) or two strands (red curve) from duplex target 16D at different values of pH. (a) DNA sequences for TFO-C used in parts b–d; (b) heating curves for measurements at pH 5.0, (c) at pH 6.0; (d) comparison of triplex measurements at three values of pH. (e) DNA sequences for TFO-C<sub>L</sub> used in parts f–h; (f) heating curves for measurements at pH 5.0, (g) at pH 6.0; (h) comparison of thermal transitions for triplexes at different pH values. Before the first cycle, the samples were annealed. For all measurements, liposomes with Ø of ~65 nm (0.5 mM POPC) and 100 nM of oligonucleotides were used, except for measurements with three strands, where 150 nM of the TFO was added.

synthesized and modified with membrane anchors, namely, a cytidine rich sequence<sup>29,40–43</sup> (TFO-C) and a guanine rich sequence (TFO-G),<sup>29,40,43</sup> which both are known to form triplexes with the PPT and to bind parallel to the duplex.<sup>29,40</sup> In

addition, TFOs with similar sequences but with locked nucleic acid (LNA) thymidines (T<sup>L</sup>) inserted in the sequence were synthesized (TFO-C<sub>L</sub> and TFO-G<sub>L</sub>) (Scheme 1), as LNA is known to increase the stability of triple helices.<sup>10,40,42,44</sup>

The ability of the modified TFOs to induce liposome assembly by formation of triple helices was tested by mixing the appropriate DNA-strands with liposomes ( $\varnothing \sim 65$  nm), annealing the sample, and monitoring the apparent absorption as a function of temperature at 260 nm. As liposome aggregates scatter the light considerably more than individual liposomes, less light will reach the detector, and as a result, the sample will have a large apparent absorbance compared to the individual liposomes.

When the sample is heated to a temperature above the denaturation temperature of the DNA-structure linking the liposomes, the aggregates break down to individual liposomes, and the apparent absorbance decreases.<sup>25,26</sup> Thermal transitions will only be observed when structures containing the lipid-modified TFO melt and consequently release the other strand(s) from the TFO.

For this reason, the breakdown of other structures, e.g., the melting of the unmodified duplex or of structures resulting from self-association of unmodified single strands, which can complicate the analysis of conventional thermal denaturation experiments with triplexes, will not obscure the thermal dissociation curves. For the data presented here, 100 nM of the DNA duplex and 150 nM of the TFO were used. Experiments with only half the concentrations gave the same results, but with reduced apparent absorbance. In contrast to other experiments involving triplex formation, measurements were started as soon as the oligonucleotides and liposomes were mixed together, without a delay for hours or days or prolonged cooling for hybridization to occur. Only a relatively fast annealing step followed by 30 min at 15 °C was performed before the actual measurements.

A transition was observed when the short duplex **16D** and **TFO-C** were mixed with liposomes and heated at pH 5.0 and 6.0. However, when the same samples were cooled and heated again, an even larger difference in the apparent absorbance between the aggregates and the liposomes was seen, i.e., the observed transition of the thermal dissociation curve became even more pronounced when the samples were heated a second time (Figure 2b,c). Cooling and heating the samples a third time did not result in any further changes, indicating that the equilibrium was reached within two cycles (Supporting Information). The need for repeated heating and cooling cycles before equilibrium is reached can be caused by the formation of competing structures due to self-association of one of the strands and indicates that some preorganization of the system is necessary. The same phenomenon has been observed to a much smaller extent for DNA-controlled assembly of liposomes by duplex formation.<sup>25</sup> The observed transitions demonstrate the feasibility of liposome aggregation controlled by the formation of triple helices, even though this requires the liposomes to be relatively close to each other and held together by a complex nucleic acid structure. The enormous steric demands of the triplex structures as interliposomal linkers and the accumulation of charged oligonucleotides are no hindrance for the reversible formation of liposome aggregates. Furthermore, the drastic change in the apparent absorbance associated with the assembly of liposomes allows detection at nanomolar DNA concentrations using a standard UV/vis spectrophotometer. The hydrophobic modification, X, does not influence the ability of the oligonucleotides to form triple helices (which was also observed for conventional thermal denaturation experiments in the absence of liposomes, Supporting Information) and liposome aggregation is not impeded by

the often slow kinetics of triplex formation.<sup>45–47</sup> To verify that the observed transitions were due to liposome assembly controlled by triplex formation and not a result of formation of other structures, experiments were carried out with the modified TFOs alone and together with only one strand of the duplex. As expected, no transitions were seen for any of the TFOs in the absence of other oligonucleotide strands, consistent with results obtained for other lipid-modified strands.<sup>25</sup> However, for the C-rich TFO (**TFO-C**), transitions of lower apparent absorbance were observed when the purine-rich strand from the duplex **16D** (5'-AAAAGAAAAGGGG-GGA) was present at pH 5.0 (Figure 2b) (equimolar concentrations of the strands were used) and to a lesser extent at pH 6.0 (Figure 2c). This finding was unexpected, but can be due to the formation of a parallel duplex<sup>16,48,49</sup> which can apparently also be used for liposome assembly.

The assembly of gold nanoparticles using only two of the strands from a triple helix has previously been observed and was ascribed to the similarities of two of the sequences used (sequence overlap),<sup>34</sup> and this could also be the case in this setup, i.e., two TFO strands could form a triple helix together with the unmodified purine-rich strand (two lipid-modified complementary strands can also cause liposome aggregation, unpublished results) (Supporting Information). However, since the similarities between the TFO and the pyrimidine-rich strand of the duplex (3'-TTTCTTTTCCCCCT) consist of a maximum of nine nucleosides and the melting temperature of the formed structure is very similar to the dissociation temperature of the structure formed with the full duplex **16D** (Figure 2b), this indicates that the same base pairs (or base pairs of similar strength) are responsible for both structures. The melting temperatures for parallel duplexes have however been found to be lower than the melting temperature for the corresponding triplexes.<sup>16</sup> At pH 6.0, the transition observed with only two strands was less pronounced and occurred at a lower temperature than at the lower pH (Figure 2b,c) which indicates that protonation of cytidines is required for the formation, consistent with the formation of Hoogsteen base pairs and a parallel duplex.<sup>48,49</sup> As expected, no significant thermal transitions were observed at pH 7.2, as cytidines need to be protonated for the TFO to be able to form a triplex.<sup>27,29</sup> Comparison of the thermal dissociation curves (heating curves) for the triple helix at the three values of pH (Figure 2d) clearly shows that the thermal dissociation temperature (melting temperature) of the structure is pH dependent and is stabilized at lower pH.<sup>29</sup>

The corresponding LNA-modified TFO, **TFO-C<sub>L</sub>**, was also able to induce liposome aggregation by triplex formation at pH 5.0 and 6.0, but for this LNA-modified TFO, the formation of a parallel duplex was less significant (Figure 2f,g). This can be due to introduction of LNA, as LNA-containing triple helices are structurally different from triple helices consisting of only DNA nucleotides.<sup>42,50,51</sup> At pH 6.0, the formation of a structure consisting of only two strands was also insignificant compared to the transition observed at pH 5.0 and especially to the thermal transition for the triple helix (Figure 2g). Also for this TFO, only a very weak transition was observed at pH 7.2 and the thermal dissociation temperature again proved to be inversely dependent on pH (Figure 2h). Comparison of the thermal dissociation curves for **TFO-C** and **TFO-C<sub>L</sub>** show that incorporation of LNA nucleotides increase the dissociation temperature as reported in the literature.<sup>40,42</sup>

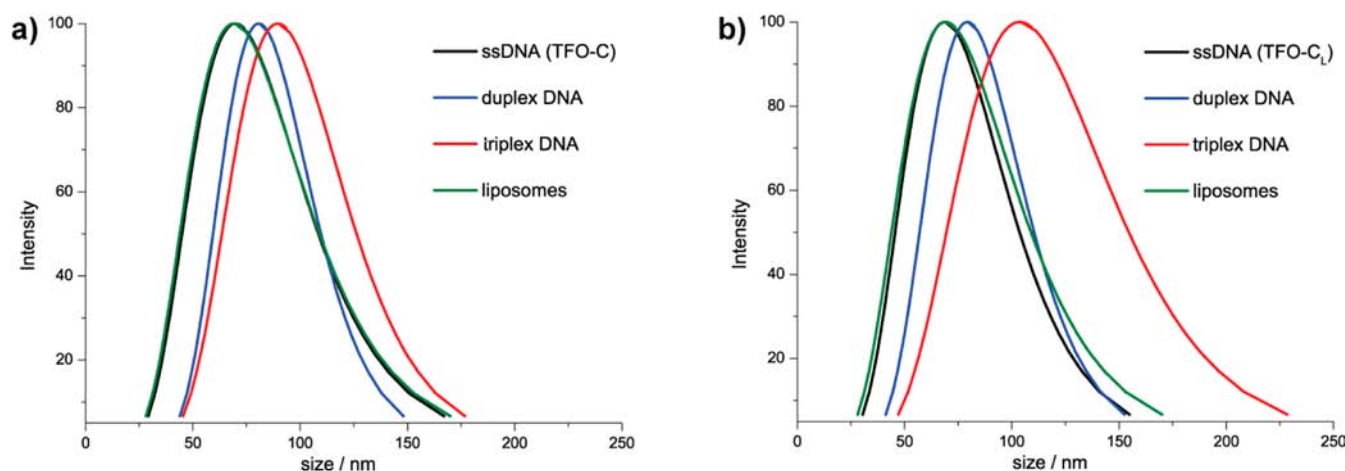


**Figure 3.** Size distribution for liposomes and liposome aggregates at pH 5.0 determined by DLS for TFO-C (a) and TFO-C<sub>L</sub> (b). Before DLS measurements, the samples had been repeatedly heated and cooled three times as described for samples used for UV spectroscopy. For all measurements, liposomes with  $\varnothing$  of  $\sim 65$  nm (0.5 mM POPC) and 100 nM of oligonucleotides were used, except for measurements with three strands, where 150 nM of the TFO was added.

For clarity, only the heating steps from the measurements are shown in the above figures, but the cooling steps often resulted in a transition at a lower temperature. This hysteresis may indicate that the system was not in equilibrium, but is more likely a result of the different processes causing the transitions: when the samples are cooled, the triplexes and consequently also liposome aggregates are formed, but when the samples are heated, the aggregates break down in a highly cooperative process,<sup>53</sup> whereas reassembly will be at a slower rate and with a much broader transition compared to the disassembly (melting) process. However, the same dissociation temperature was always observed using the same heating or cooling rate. As for liposome aggregation caused by the formation of double helices,<sup>25,26</sup> the observed thermal transitions are very sharp compared to conventional thermal denaturation experiments without liposomes.<sup>1</sup> Sharp thermal transitions have also been reported for assemblies of DNA-functionalized gold nanoparticles<sup>52</sup> and were ascribed to a cooperative process resulting from several DNA strands linking the nanoparticles and the change in local salt concentration upon melting.<sup>53</sup> The same observations are likely to be valid for the system described here; the thermal dissociation results in sharp transitions of the heating curves, as the initial melting of the DNA-linkers destabilizes the remaining DNA-linkers and thereby accelerates disassembly of the aggregates. The melting temperature is decreased during melting for the remaining DNA-linkers due to a decrease in the local salt concentration.<sup>53</sup> Furthermore, the dispersion of the nanoparticles/liposomes, which are forced close together ( $\sim 5$  nm) in the assemblies, is another contributing factor. The lower concentration limit for the formation of liposome aggregates by triple helical oligonucleotide linkers depends on the dissociation constants of the respective triple helix. A solution of extruded POPC liposomes (1 mL, 65 nm size, 0.05 mM POPC) contains about  $1.17 \times 10^{11}$  liposomes (polydispersity is not taken into account) and, on average, 515 TFO-probe strands are anchored to each liposome assuming an equal statistical distribution (100 nM DNA concentration; for equations used, see Supporting Information). Assuming a typical dissociation constant for triplex formation in the low micromolar range (e.g., 5  $\mu$ M), only 2% triplex formation is required to achieve liposome assembly at 100 nM TFO probe concentration, which

corresponds to an average of 10 triple helices linking two liposomes. The influence of the dissociation constants can be seen for TFO-C compared to the LNA-modified TFO-C<sub>L</sub>; TFO-C<sub>L</sub> shows a sharper melting transition than TFO-C, which is assumed to correspond to a larger number of triple helical linkers between two liposomes which is consistent with LNA's ability to stabilize triple helices with a lower dissociation constant.<sup>40</sup> The broader transitions for TFO-C are consistent with the model from Schatz et al. which has shown that assemblies of gold nanoparticles become much broader with a decreasing number of linking oligonucleotides due to the decrease in the local salt concentration.<sup>53</sup>

Conventional thermal denaturation experiments in the absence of liposomes (1  $\mu$ M DNA was used, except for measurements with three strands where 1.5  $\mu$ M of the TFO was added) revealed more complex transitions for the chosen sequences, as not only were parallel duplexes observed, but for both TFO-C and the strand from the duplex with a similar sequence (5'-TTTTCTTTTCCCCCT), thermal transitions were observed for the single strands (i.e., when no other DNA strands were present). This was not seen for TFO-C<sub>L</sub>, but was not unexpected, as the C-rich sequence has been reported to self-associate,<sup>43</sup> probably due to the formation of an i-motif.<sup>21,22,43</sup> The formed "structure" was dependent on protonation of the cytidines and had a higher melting temperature at low values of pH (Table 1, Supporting Information), as observed for i-motifs.<sup>11,21,22</sup> However, no transition was seen in thermal denaturation experiments with liposomes (Figure 2b,c), suggesting that the formed structures are not able to induce liposome assembly or that the self-association of the oligonucleotide does not happen at the 10–20-fold lower concentration used for liposome experiments as compared to the standard thermal denaturation experiments. This observation suggests a further advantage of the low nanomolar concentrations which is sufficient for these experiments, as the (intermolecular) self-association of oligonucleotides can be less pronounced at low concentrations.<sup>18</sup>

It is a clear advantage over conventional thermal denaturation analysis that self-aggregation of single-stranded sequences or the formation of other structures of higher order (e.g., the duplex to single strand transition), which do not involve the



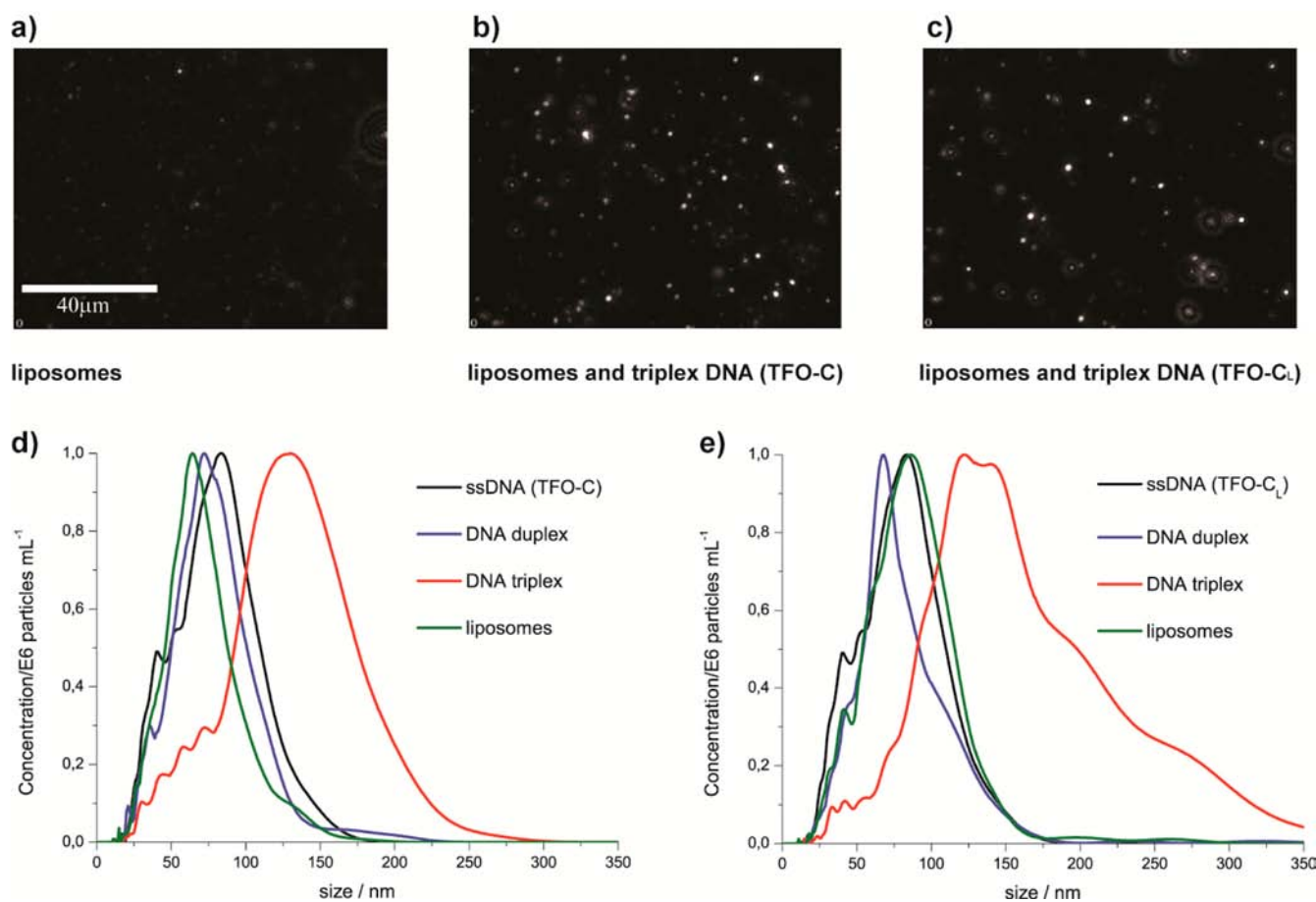


**Figure 4.** Liposome assembly monitored by NTA at pH 5.0. (a–c) Snapshots from videos used for nanoparticle tracking analysis of liposomes without added nucleotides (a), liposomes with TFO-C and duplex 16D (b), and liposomes with TFO-C<sub>L</sub> and duplex 16D (c), (d,e) particle-size distribution profiles of liposomes and liposome aggregates for TFO-C and TFO-C<sub>L</sub>, respectively, (normalized data) at pH 5.0 as measured by nanoparticle tracking analysis. Before NTA measurements, the samples were repeatedly heated and cooled three times as described for samples used for UV spectroscopy. For all measurements, liposomes with  $\varnothing$  of  $\sim 65$  nm were used. 5 nM oligonucleotides and 0.025 mM POPC were used for samples containing one or two strands, whereas 2 nM duplex, 3 nM TFO, and 0.01 mM POPC were used for measurements with three strands.

TFO, do not obscure the thermal denaturation analysis during triplex-controlled assembly of liposomes. Furthermore, by this method it is possible to investigate the formation and behavior of triple helices at low nanomolar DNA concentrations as the aggregate dissociation is accompanied by a large decrease in signal intensity. The observed transitions therefore are due to the difference in size between the individual liposomes and the liposome aggregates<sup>25,26</sup> and not the change in absorbance accompanying duplex denaturation like in conventional thermal denaturation experiments.<sup>1,54</sup> Even though the thermal dissociation processes are monitored at 260 nm, the concentration of DNA in the samples is too low to be detected in these experiments.<sup>25,26</sup> As the apparent change in absorption is due to light scattering, it is possible to monitor the assembly/disassembly process at a broader range of wavelengths than can be used for conventional thermal denaturation experiments. Moreover, the thermal dissociation curves are reversed as compared to conventional thermal denaturation profiles,<sup>25,26</sup> which makes it easy to distinguish the different transitions. In addition to UV-spectroscopy, two independent and complementary methods were used to analyze the aggregate formation; Dynamic light scattering (DLS) is an established method for bulk analysis of liquid samples and measures the fluctuations in the intensity of the light scattered from the particles in a sample due to their Brownian motion,<sup>55</sup> whereas

nanoparticle tracking analysis (NTA) is a single particle tracking method which relies on the light scattered from individual particles to track the displacement (in two dimensions) due to the Brownian motion of each particle.<sup>56,57</sup>

Both methods then use the Stokes–Einstein equation to calculate the hydrodynamic diameter of the particles, but whereas the output from DLS is an intensity based size distribution,<sup>55</sup> NTA gives a particle size distribution based on the number of observed particles.<sup>56</sup> The formation of liposome aggregates was tested by DLS for TFO-C and TFO-C<sub>L</sub> at pH 5.0 (Figure 3). For both TFOs, no difference in the size distribution between liposomes without added oligonucleotides and liposomes in the presence of TFO (green and black curves, respectively) was seen, again demonstrating that liposome aggregation cannot be induced by the single stranded TFOs alone. When the purine-rich strand of the duplex was present, the measured average particle size was increased (blue curve) indicating the formation of liposome aggregates due to the formation of a parallel duplex. However, even larger aggregates were formed with the full duplex (red curve), further supporting the proposed liposome assembly by triple helix formation. Whereas samples used for UV-spectroscopic measurements could also be used for DLS measurements, dilution (20- or 50-fold depending on the nature of the sample) of samples used for thermal denaturation experiments was

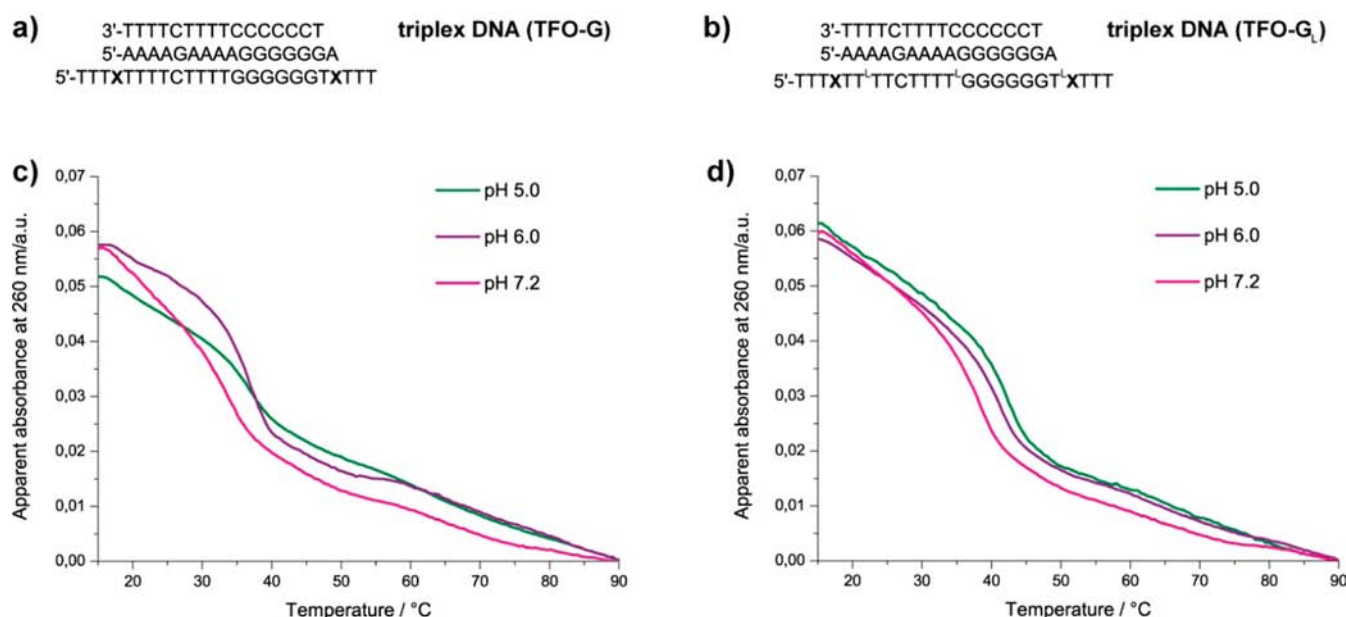


**Figure 5.** (a,b) Sequences for the strands used to form a triple helix for TFO-G and TFO-G<sub>L</sub>, respectively; (c,d) first heating curve for triple helix-mediated liposome aggregates formed with TFO-G and TFO-G<sub>L</sub>, respectively, at different pH values. For all measurements, liposomes with Ø of ~65 nm (0.5 mM POPC) and 100 nM of oligonucleotides were used, except for measurements with three strands, where 150 nM of the TFO was added.

necessary prior to NTA due to the greater sensitivity of this method. NTA allows exclusion of “large dust particles” by visual inspection of the area which is measured, and very large particles were avoided. When this method was used on samples with similar ratios of liposomes and oligonucleotides as used for UV-spectroscopy and DLS (i.e., an effective excess of liposomes as compared to oligonucleotides), no significant difference in the measured sizes was seen between the liposomes and the structures formed when DNA-strands were added. The reason for this is that DLS is not able to differentiate mixtures of particles of very similar sizes and the result for the average size will then be shifted toward the size of the larger particles, as these scatter the light more intensely;<sup>58</sup> i.e., this bias makes the aggregates easier to see with DLS, whereas in NTA, the larger population of smaller particles (liposomes which have not aggregated) are more clearly seen, as this technique relies on the light scattered from individual particles and hence on the number of particles and not on the intensity of the scattered light (except the minimal intensity of scattered light required to localize the individual particle). For this reason, the excess of liposomes in the samples was reduced by using only one-tenth of the amount used for UV-spectroscopy and DLS measurements to ensure that the majority of liposomes in the samples would participate in aggregation. Using these samples, a significant increase in size between liposomes alone and liposomes in the presence of triple helix formation was clearly seen for both TFO-C (Figure 4d) and TFO-C<sub>L</sub> (Figure 4f), again substantiating the DNA-controlled assembly of liposomes. The small difference in hydrodynamic radius in combination with the uncertainty in the NTA measurements does not allow distinguishing between liposomes without oligonucleotides or with TFO and only one of the strands from the duplex target (Figure 4d,e). However, an increase in particle size was seen when a triple helix was present, enabling the detection of triple helix formation at a concentration of only 2 nM of the duplex target. The detection limit for hybridization

of oligonucleotides forming triple helices using liposomes and NTA is thereby in the low nanomolar concentration range, which is 1000 times less than usually used for regular thermal denaturation analysis by UV-spectroscopy without liposomes.

The differences in the average particle sizes between the samples were also easily observed visually by looking at videos recorded by the NTA camera system (Figure 4a–c). Whereas only small particles were seen in all samples of liposomes containing no (Figure 4a), one, or two DNA strands (Supporting Information), larger particle aggregates were easily seen for samples containing the full triple helix (Figure 4b,c).

For the G-rich TFOs, no transitions were observed for the single stranded TFO-G, TFO-G<sub>L</sub> or the similar unmodified strand in ordinary thermal denaturation experiments without liposomes (micromolar concentrations), even though this sequence (modified with 5-methyl-2'-deoxycytidine) has been reported to self-aggregate.<sup>43</sup> In addition, no transitions were seen for the lipid-modified TFOs alone in thermal denaturation experiments with liposomes and no significant transitions were seen in thermal denaturation experiments with liposomes in the absence of the purine-rich strand (5'-TTTCTTTCCCCCT) for neither of the modified TFOs at any pH value (Supporting Information), suggesting that neither TFO-G or TFO-G<sub>L</sub> are able to form a parallel duplex as observed for TFO-C. However, transitions were observed for both TFOs when the unmodified double helix was added (Figure 5c,d). For this TFO-sequence, repeated heating and cooling of the samples did not result in transitions of a higher intensity as was observed for both the cytidine-rich TFOs, which is assumed to be the result of different stability of the formed triple helix or because no other structures (e.g., i-motifs and parallel duplexes) are competing for the formation of triplexes, as both the sequence of the TFO<sup>46</sup> and the formation of secondary structures by TFOs can influence the kinetics of the triplex formation.<sup>46</sup> Since the guanine-rich TFOs are not dependent on protonation of cytidine, transitions were observed at all tested pH values, and



as reported in the literature, the melting/dissociation temperature showed only a negligible pH dependence.<sup>29</sup> As seen for the C-rich TFOs, the dissociation temperature was increased by incorporation of LNA nucleotides.<sup>40</sup>

A current limitation of the system described here is that apparently duplex targets much longer than the modified TFO are not tolerated, as no transitions were observed for any of the four TFOs in thermal denaturation experiments with liposomes with the long duplex target (47D). This finding was expected and substantiates the proposed mechanism of DNA-controlled liposome assembly, as the absence of transitions can be attributed to the inability of the long, rigid duplex to be positioned between two liposomes upon assembly due to steric hindrance and accumulation of negative charge.

## CONCLUSION

In conclusion, the assembly of liposomes controlled by the formation of triple helices was shown by three different analytical methods, all taking advantage of the differences in size between liposomes and liposome aggregates and the subsequent changes in the optical properties or speed of diffusion (NTA). The assembly was demonstrated by the use of different triplex forming oligonucleotides which were modified at both ends with lipophilic substituents (membrane anchors). The modifications did not influence the ability of the oligonucleotides to form triple helices, and as the principle is based on noncovalent hydrophobic interactions, no surface chemistry or other synthetic procedures for coupling of DNA to the nanoparticles or subsequent purification were necessary. All tested TFOs were able to induce assembly of liposomes, and it was found that insertion of LNA in the TFO can be favorable and suppresses the formation of other structures for some TFO-sequences, as the insertion of LNA favored the formation of triplexes compared to parallel duplexes for the cytidine-rich TFO-sequence, whereas no significant effect of the insertion of LNA was observed for the guanine-rich sequence. The presented assembly based on the formation of triple helices is a very fast process, and the measurements can be started as soon as the oligonucleotides and liposomes are mixed together without the need for a long initial cooling period. The triplex-mediated assembly of liposomes can be an advantage as only structures involving the modified TFO give rise to transitions in thermal denaturation experiments and the spectra are therefore not obscured by other transitions or features, including the melting transition of the unmodified double helix or structures formed by the self-aggregation of single strands. Moreover, this method allows the study of triple helix formation at low nanomolar concentrations of DNA; however, the currently used TFO-probes do not allow targeting of double stranded oligonucleotides which are much longer than the probe strand. Furthermore, this method allows hybridization experiments involving triple helices ( $T_m$  measurements) to be performed at a broad range of wavelengths, as the observed change in absorbance is due to the scattering of light by the liposome aggregates during assembly and disassembly of liposomes and not the specific absorption maximum of DNA used in conventional thermal denaturation analysis. The results also show that it is possible to use the DNA-controlled assembly of liposomes to target double stranded stretches of DNA by using the duplex as target in triple helix formation.

## ASSOCIATED CONTENT

### Supporting Information

Thermal denaturation measurements for oligonucleotides with and without liposomes, additional dynamic light scattering (DLS), MALDI-TOF data for oligonucleotides and nanoparticle tracking analysis (NTA) data. This material is available free of charge via the Internet at <http://pubs.acs.org>.

## AUTHOR INFORMATION

### Corresponding Author

\*E-mail: [snv@sdu.dk](mailto:snv@sdu.dk).

### Notes

The authors declare no competing financial interest.

## ACKNOWLEDGMENTS

This work has been supported by the Nucleic Acid Center funded by the Danish National Research Foundation and BioNEC, a centre of Excellence funded by THE VILLUM FOUNDATION for studies on biomolecular nanoscale engineering.

## REFERENCES

- (1) Mergny, J.-L., and Lacroix, L. (2003) Analysis of thermal melting curves. *Oligonucleotides* 13, 515–537.
- (2) Vossen, R. H. A. M., Aten, E., Roos, A., and den Dunnen, J. T. (2009) High-resolution melting analysis (HRMA)-more than just sequence variant screening. *Hum. Mutat.* 30, 860–866.
- (3) Farrar, J. S. R., Gudrun, H.; Wittwer, C. T. (2009) High-resolution melting curve analysis for molecular diagnostics, In *Molecular Diagnostics* (Patrinou, G. P., and Ansong, W. J., Eds.) pp 229–245, Academic Press, Burlington, MA.
- (4) Rosi, N. L., and Mirkin, C. A. (2005) Nanostructures in biodiagnostics. *Chem. Rev.* 105, 1547–1562.
- (5) Keer, J. C. (2008) Quantitative Real-time PCR Analysis, In *Essentials of Nucleic Acid Analysis: A Robust Approach* (Keer, J. T., and Birch, L., Eds.) pp 132–166, Chapter 7, RSC Publishing, Cambridge.
- (6) Arimondo, P. B., Barcelo, F., Sun, J. S., Maurizot, J. C., Garestier, T., and Helene, C. (1998) Triple helix formation by (G,A)-containing oligonucleotides: asymmetric sequence effect. *Biochemistry* 37, 16627–16635.
- (7) Arimondo, P. B., Garestier, T., Helene, C., and Sun, J. S. (2001) Detection of competing DNA structures by thermal gradient gel electrophoresis: from self-association to triple helix formation by (G,A)-containing oligonucleotides. *Nucleic Acids Res.* 29, E15.
- (8) Jetter, M. C., and Hobbs, F. W. (1993) 7,8-Dihydro-8-oxoadenine as a replacement for cytosine in the third strand of triple helices. Triplex formation without hypochromicity. *Biochemistry* 32, 3249–3254.
- (9) Faucon, B., Mergny, J. L., and Helene, C. (1996) Effect of third strand composition on the triple helix formation: purine versus pyrimidine oligodeoxynucleotides. *Nucleic Acids Res.* 24, 3181–3188.
- (10) Obika, S., Uneda, T., Sugimoto, T., Nanbu, D., Minami, T., Doi, T., and Imanishi, T. (2001) 2'-O,4'-C-methylene bridged nucleic acid (2'-4'-BNA): Synthesis and triplex-forming properties. *Bioorg. Med. Chem.* 9, 1001–1011.
- (11) Lacroix, L., and Mergny, J. L. (2000) Chemical modification of pyrimidine TFOs: Effect on i-motif and triple helix formation. *Arch. Biochem. Biophys.* 381, 153–163.
- (12) Svinarchuk, F., Monnot, M., Merle, A., Malvy, C., and Femandjian, S. (1995) The high stability of the triple helices formed between short purine oligonucleotides and SIV/HIV-2 vpx genes is determined by the targeted DNA structure. *Nucleic Acids Res.* 23, 3831–3836.
- (13) Svinarchuk, F., Debin, A., Bertrand, J. R., and Malvy, C. (1996) Investigation of the intracellular stability and formation of a triple helix

formed with a short purine oligonucleotide targeted to the murine c-pim-1 proto-oncogene promoter. *Nucleic Acids Res.* 24, 295–302.

(14) Alunni-Fabbroni, M., Pirulli, D., Manzini, G., and Xodo, L. E. (1996) (A,G)-oligonucleotides form extraordinary stable triple helices with a critical RY sequence of the murine c-Ki-ras promoter and inhibit transcription in transfected NIH 3T3 cells. *Biochemistry* 35, 16361–16369.

(15) Svinarchuk, F., Paoletti, J., and Malvy, C. (1995) An unusually stable purine(purine-pyrimidine) short triplex. The third strand stabilizes double-stranded DNA. *J. Biol. Chem.* 270, 14068–14071.

(16) Globisch, D., Bomholt, N., Filichev, V. V., and Pedersen, E. B. (2008) Stability of Hoogsteen-type triplexes - Electrostatic attraction between duplex backbone and triplex-forming oligonucleotide (TFO) using an intercalating conjugate. *Helv. Chim. Acta* 91, 805–818.

(17) Roberts, R. W., and Crothers, D. M. (1991) Specificity and stringency in DNA triplex formation. *Proc. Natl. Acad. Sci. U.S.A.* 88, 9397–9401.

(18) Alunni-Fabbroni, M., Manzini, G., Quadrioglio, F., and Xodo, L. E. (1996) Guanine-rich oligonucleotides targeted to a critical R. Y site located in the Ki-ras promoter. The effect of competing self-structures on triplex formation. *Eur. J. Biochem.* 238, 143–151.

(19) Svinarchuk, F., Cherny, D., Debin, A., Delain, E., and Malvy, C. (1996) A new approach to overcome potassium-mediated inhibition of triplex formation. *Nucleic Acids Res.* 24, 3858–3865.

(20) Saxena, S., Bansal, A., and Kukreti, S. (2008) Structural polymorphism exhibited by a homopurine.homopyrimidine sequence found at the right end of human c-jun protooncogene. *Arch. Biochem. Biophys.* 471, 95–108.

(21) Mergny, J. L., Lacroix, L., Han, X. G., Leroy, J. L., and Helene, C. (1995) Intramolecular Folding of Pyrimidine Oligodeoxynucleotides into an I-DNA Motif. *J. Am. Chem. Soc.* 117, 8887–8898.

(22) Lacroix, L., Mergny, J. L., Leroy, J. L., and Helene, C. (1996) Inability of RNA to form the i-motif: Implications for triplex formation. *Biochemistry* 35, 8715–8722.

(23) Noonberg, S. B., Francois, J. C., Garestier, T., and Helene, C. (1995) Effect of competing self-structure on triplex formation with purine-rich oligodeoxynucleotides containing GA repeats. *Nucleic Acids Res.* 23, 1956–1963.

(24) Noonberg, S. B., Francois, J. C., Praseuth, D., Guieysse-Peugeot, A. L., Lacoste, J., Garestier, T., and Helene, C. (1995) Triplex formation with alpha anomers of purine-rich and pyrimidine-rich oligodeoxynucleotides. *Nucleic Acids Res.* 23, 4042–4049.

(25) Jakobsen, U., Simonsen, A. C., and Vogel, S. (2008) DNA-controlled assembly of soft nanoparticles. *J. Am. Chem. Soc.* 130, 10462–10463.

(26) Jakobsen, U., and Vogel, S. (2009) Chapter 12 - DNA-controlled assembly of liposomes in diagnostics. *Methods Enzymol.* 464, 233–248.

(27) Soyfer, V. N., and Potaman, V. N. (1996) *Triple-Helical Nucleic Acids*, Springer, New York.

(28) Robles, J., Grandas, A., Pedrosa, E., Luque, F. J., Eritja, R., and Orozco, M. (2002) Nucleic acid triple helices: Stability effects of nucleobase modifications. *Curr. Org. Chem.* 6, 1333–1368.

(29) Giovannangeli, C., Rougee, M., Garestier, T., Thuong, N. T., and Helene, C. (1992) Triple-helix formation by oligonucleotides containing the three bases thymine, cytosine, and guanine. *Proc. Natl. Acad. Sci. U.S.A.* 89, 8631–8635.

(30) Sun, J. S., De Bizemont, T., Duval-Valentin, G., Montenay-Garestier, T., and Helene, C. (1991) Extension of the range of recognition sequences for triple helix formation by oligonucleotides containing guanines and thymine. *C. R. Acad. Sci. III* 313, 585–590.

(31) Jung, Y. H., Lee, K. B., Kim, Y. G., and Choi, I. S. (2006) Proton-fueled, reversible assembly of gold nanoparticles by controlled triplex formation. *Angew. Chem., Int. Ed.* 45, 5960–5963.

(32) Murphy, D., Eritja, R., and Redmond, G. (2004) Monitoring denaturation behaviour and comparative stability of DNA triple helices using oligonucleotide-gold nanoparticle conjugates. *Nucleic Acids Res.* 32, e65.

(33) McKenzie, F., Faulds, K., and Graham, D. (2008) LNA functionalized gold nanoparticles as probes for double stranded DNA through triplex formation. *Chem. Commun.*, 2367–2369.

(34) Han, M. S., Lytton-Jean, A. K. R., and Mirkin, C. A. (2006) A gold nanoparticle based approach for screening triplex DNA binders. *J. Am. Chem. Soc.* 128, 4954–4955.

(35) Qu, X. G., Zhao, C., Qu, K. G., Xu, C., and Ren, J. S. (2011) Triplex inducer-directed self-assembly of single-walled carbon nanotubes: a triplex DNA-based approach for controlled manipulation of nanostructures. *Nucleic Acids Res.* 39, 3939–3948.

(36) Yoshina-Ishii, C., and Boxer, S. G. (2003) Arrays of mobile tethered vesicles on supported lipid bilayers. *J. Am. Chem. Soc.* 125, 3696–3697.

(37) Benkoski, J. J., and Höök, F. (2005) Lateral mobility of tethered vesicle - DNA assemblies. *J. Phys. Chem. B* 109, 9773–9779.

(38) Zhang, G. R., Farooqui, F., Kinstler, O., and Letsinger, R. L. (1996) Informational liposomes: Complexes derived from cholesteryl-conjugated oligonucleotides and liposomes. *Tetrahedron Lett.* 37, 6243–6246.

(39) Rohr, K., and Vogel, S. (2006) Polyaza crown ethers as non-nucleosidic building blocks in DNA conjugates: Synthesis and remarkable stabilization of dsDNA. *ChemBioChem* 7, 463–470.

(40) Brunet, E., Alberti, P., Perrouault, L. C., Babu, R., Wengel, J., and Giovannangeli, C. (2005) Exploring cellular activity of locked nucleic acid-modified triplex-forming oligonucleotides and defining its molecular basis. *J. Biol. Chem.* 280, 20076–20085.

(41) Teulade-Fichou, M. P., Perrin, D., Bourtoune, A., Polverari, D., Vigneron, J. P., Lehn, J. M., Sun, J. S., Garestier, T., and Helene, C. (2001) Direct photocleavage of HIV-DNA by quinacridine derivatives triggered by triplex formation. *J. Am. Chem. Soc.* 123, 9283–9292.

(42) Sun, B. W., Babu, B. R., Sorensen, M. D., Zakrzewska, K., Wengel, J., and Sun, J. S. (2004) Sequence and pH effects of LNA-containing triple helix-forming oligonucleotides: physical chemistry, biochemistry, and modeling studies. *Biochemistry* 43, 4160–4169.

(43) Capobianco, M. L., De Champdore, M., Arcamone, F., Garbesi, A., Gulancvarc'h, D., and Arimondo, P. B. (2005) Improved synthesis of daunomycin conjugates with triplex-forming oligonucleotides. The polypurine tract of HIV-1 as a target. *Bioorgan. Med. Chem.* 13, 3209–3218.

(44) Obika, S., Hari, Y., Sugimoto, T., Sekiguchi, M., and Imanishi, T. (2000) Triplex-forming enhancement with high sequence selectivity by single 2'-O,4'-C-methylene bridged nucleic acid (2',4'-BNA) modification. *Tetrahedron Lett.* 41, 8923–8927.

(45) Xodo, L. E. (1995) Kinetic analysis of triple-helix formation by pyrimidine oligodeoxynucleotides and duplex DNA. *Eur. J. Biochem.* 228, 918–926.

(46) Paes, H. M., and Fox, K. R. (1997) Kinetic studies on the formation of intermolecular triple helices. *Nucleic Acids Res.* 25, 3269–3274.

(47) Rougee, M., Faucon, B., Mergny, J. L., Barcelo, F., Giovannangeli, C., Garestier, T., and Helene, C. (1992) Kinetics and thermodynamics of triple-helix formation: effects of ionic strength and mismatches. *Biochemistry* 31, 9269–9278.

(48) Liu, K. L., Miles, H. T., Frazier, J., and Sasisekharan, V. (1993) A novel DNA duplex - a parallel-stranded DNA helix with Hoogsteen base-pairing. *Biochemistry* 32, 11802–11809.

(49) Cubero, E., Avino, A., de la Torre, B. G., Frieden, M., Eritja, R., Luque, F. J., Gonzalez, C., and Orozco, M. (2002) Hoogsteen-based parallel-stranded duplexes of DNA. Effect of 8-amino-purine derivatives. *J. Am. Chem. Soc.* 124, 3133–3142.

(50) Sorensen, J. J., Nielsen, J. T., and Petersen, M. (2004) Solution structure of a dsDNA:LNA triplex. *Nucleic Acids Res.* 32, 6078–6085.

(51) Torigoe, H., Hari, Y., Sekiguchi, M., Obika, S., and Imanishi, T. (2001) 2'-O,4'-C-methylene bridged nucleic acid modification promotes pyrimidine motif triplex DNA formation at physiological pH: thermodynamic and kinetic studies. *J. Biol. Chem.* 276, 2354–2360.

(52) Elghanian, R., Storhoff, J. J., Mucic, R. C., Letsinger, R. L., and Mirkin, C. A. (1997) Selective colorimetric detection of polynucleo-

tides based on the distance-dependent optical properties of gold nanoparticles. *Science* 277, 1078–1081.

(53) Jin, R. C., Wu, G. S., Li, Z., Mirkin, C. A., and Schatz, G. C. (2003) What controls the melting properties of DNA-linked gold nanoparticle assemblies? *J. Am. Chem. Soc.* 125, 1643–1654.

(54) Tinoco, I. (1960) Hypochromism in polynucleotides. *J. Am. Chem. Soc.* 82, 4785–4790.

(55) Merkus, H. G. (2009) *Particle Size Measurements*, Springer.

(56) Malloy, A., and Carr, B. (2006) Nanoparticle tracking analysis - The Halo (TM) system. *Part. Part. Syst. Char.* 23, 197–204.

(57) (2009) Applications of Nanoparticle Tracking Analysis (NTA) in Nanoparticle Research, 26/11/2009 ed., [www.nanosight.com](http://www.nanosight.com).

(58) Filipe, V., Hawe, A., and Jiskoot, W. (2010) Critical evaluation of nanoparticle tracking analysis (NTA) by nanosight for the measurement of nanoparticles and protein aggregates. *Pharm. Res.* 27, 796–810.

(59) Dave, N., and Liu, J. (2011) Programmable assembly of DNA-functionalized liposomes by DNA. *ACS Nano* 5, 1304–1312.

(60) Gosse, C., Boutorine, A., Aujard, I., Chami, M., Kononov, A., Cogne-Laage, E., Allemand, J. F., Li, J., and Jullien, L. (2004) Micelles of lipid-oligonucleotide conjugates: Implications for membrane anchoring and base pairing. *J. Phys. Chem. B* 108, 6485–6497.

(61) Pfeiffer, I., and Höök, F. (2004) Bivalent cholesterol-based coupling of oligonucleotides to lipid membrane assemblies. *J. Am. Chem. Soc.* 126, 10224–10225.

(62) Vu, H., Schmaltz-Hill, T., and Jayaraman, K. (1994) Synthesis and properties of cholesteryl-modified triple-helix forming oligonucleotides containing a triglycyl linker. *Bioconjugate Chem.* 5, 666–668.